

---

This is an electronic reprint of the original article.  
This reprint may differ from the original in pagination and typographic detail.

Author(s): Kemppinen, Antti & Manninen, Antti J. & Möttönen, Mikko & Vartiainen, Juha J. & Peltonen, Joonas T. & Pekola, Jukka  
Title: Suppression of the critical current of a balanced superconducting quantum interference device  
Year: 2008  
Version: Final published version

**Please cite the original version:**

Kemppinen, Antti & Manninen, Antti J. & Möttönen, Mikko & Vartiainen, Juha J. & Peltonen, Joonas T. & Pekola, Jukka. 2008. Suppression of the critical current of a balanced superconducting quantum interference device. *Applied Physics Letters*. Volume 92, Issue 5. P. 052110/1-3. ISSN 0003-6951 (printed). DOI: 10.1063/1.2842413.

Rights: © 2008 AIP Publishing. This article may be downloaded for personal use only. Any other use requires prior permission of the author and the American Institute of Physics. The following article appeared in *Applied Physics Letters* and may be found at <http://scitation.aip.org/content/aip/journal/apl/92/5/10.1063/1.2842413>

---

All material supplied via Aaltodoc is protected by copyright and other intellectual property rights, and duplication or sale of all or part of any of the repository collections is not permitted, except that material may be duplicated by you for your research use or educational purposes in electronic or print form. You must obtain permission for any other use. Electronic or print copies may not be offered, whether for sale or otherwise to anyone who is not an authorised user.

## Suppression of the critical current of a balanced superconducting quantum interference device

Antti Kemppinen, Antti J. Manninen, Mikko Möttönen, Juha J. Vartiainen, Joonas T. Peltonen, and Jukka P. Pekola

Citation: *Applied Physics Letters* **92**, 052110 (2008); doi: 10.1063/1.2842413

View online: <http://dx.doi.org/10.1063/1.2842413>

View Table of Contents: <http://scitation.aip.org/content/aip/journal/apl/92/5?ver=pdfcov>

Published by the [AIP Publishing](#)

---

### Articles you may be interested in

[Nano-superconducting quantum interference devices with suspended junctions](#)

*Appl. Phys. Lett.* **104**, 152603 (2014); 10.1063/1.4871317

[Supercurrent decay in nano-superconducting quantum interference devices for intrinsic magnetic flux resolution](#)

*Appl. Phys. Lett.* **94**, 062503 (2009); 10.1063/1.3078519

[Fraunhofer regime of operation for superconducting quantum interference filters](#)

*Appl. Phys. Lett.* **93**, 262503 (2008); 10.1063/1.3058759

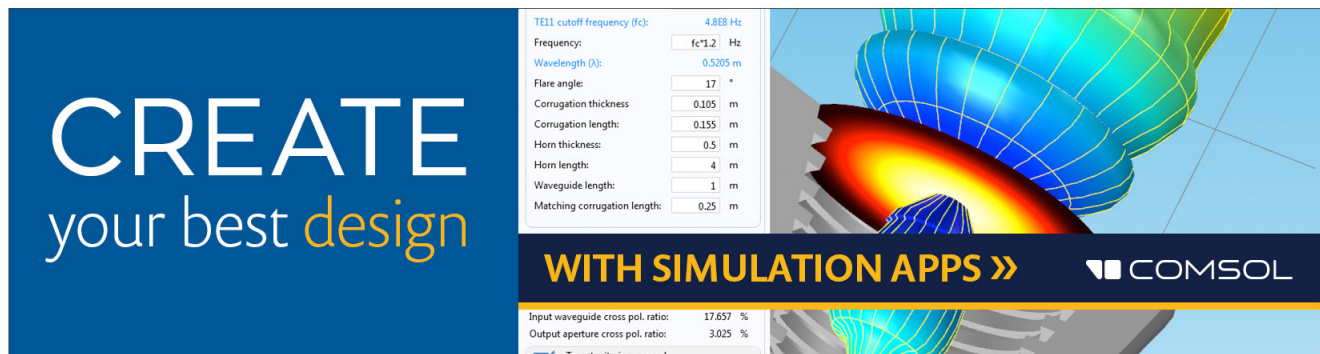
[Influence of bicrystal microstructural defects on high-transition-temperature direct-current superconducting quantum interference device](#)

*Appl. Phys. Lett.* **88**, 102504 (2006); 10.1063/1.2182066

[The current–voltage characteristics of the resistive direct current superconducting quantum interference device](#)

*J. Appl. Phys.* **81**, 2010 (1997); 10.1063/1.364057

---

The advertisement for COMSOL simulation software features a blue background on the left with the text 'CREATE your best design' in white and yellow. On the right, there is a 3D simulation of a horn antenna with a color-coded field distribution. A control panel on the left lists various parameters for a TE11 cutoff frequency, such as frequency (4.868 Hz), wavelength (0.5205 m), flare angle (17 degrees), and corrugation thickness (0.105 m). The bottom right corner displays the COMSOL logo and the text 'WITH SIMULATION APPS >>'.

TE11 cutoff frequency (fc): 4.868 Hz	
Frequency:	<input type="text" value="fc*1.2"/> Hz
Wavelength (lambda):	<input type="text" value="0.5205"/> m
Flare angle:	<input type="text" value="17"/> °
Corrugation thickness:	<input type="text" value="0.105"/> m
Corrugation length:	<input type="text" value="0.155"/> m
Horn thickness:	<input type="text" value="0.5"/> m
Horn length:	<input type="text" value="4"/> m
Waveguide length:	<input type="text" value="1"/> m
Matching corrugation length:	<input type="text" value="0.25"/> m

Input waveguide cross pol. ratio: 17.657 %  
Output aperture cross pol. ratio: 3.025 %  
 Target criterion: passed

# Suppression of the critical current of a balanced superconducting quantum interference device

Antti Kemppinen,<sup>1,a)</sup> Antti J. Manninen,<sup>1</sup> Mikko Möttönen,<sup>2,3</sup> Juha J. Vartiainen,<sup>2</sup> Joonas T. Peltonen,<sup>2</sup> and Jukka P. Pekola<sup>2</sup>

<sup>1</sup>Centre for Metrology and Accreditation (MIKES), P.O. Box 9, 02151 ESPOO, Finland

<sup>2</sup>Low Temperature Laboratory, Helsinki University of Technology, P.O. Box 3500, 02015 TKK, Finland

<sup>3</sup>Department of Engineering Physics/COMP, Helsinki University of Technology, P.O. Box 5100, 02015 TKK, Finland

(Received 12 December 2007; accepted 22 January 2008; published online 8 February 2008)

We present an experimental study of the magnetic flux dependence of the critical current of a balanced superconducting quantum interference device (SQUID) with three Josephson junctions in parallel. Unlike for ordinary direct current (dc) SQUIDs, the suppression of the critical current does not depend on the exact parameters of the Josephson junctions. The suppression is essentially limited only by the inductances of the SQUID loops. We demonstrate a critical current suppression ratio of higher than 300 in a balanced SQUID with a maximum critical current 30 nA. © 2008 American Institute of Physics. [DOI: 10.1063/1.2842413]

Direct current (dc) superconducting quantum interference devices (SQUIDs) are routinely used to provide tunable critical current  $I_c$ , e.g., in quantum computing applications.<sup>1,2</sup> For example, some charge qubits and charge pumps would benefit if  $I_c$  could be tuned very close to zero.<sup>3–5</sup> These devices require Coulomb blockade and, hence, very small Josephson junctions (JJs) must be used. The range of the critical current of a dc SQUID is  $|I_{c1} \pm I_{c2}|$ , where  $I_{ci}$  are the critical currents of the individual JJs. It is not possible to fabricate two identical junctions, hence some residual critical current always exists. As suggested in Refs. 3–5, this problem can be completely eliminated by using a balanced SQUID, i.e., a structure with three parallel JJs in two superconducting loops with individual magnetic flux controls. Surprisingly, only few experiments have utilized individual on-chip flux controls instead of a homogeneous external flux (see, e.g., Refs. 6 and 7). In this paper, we present an experimental study of the balanced SQUID. Our prime motivation to search for high critical current suppression ratio is to improve the accuracy of the Cooper pair sluice.<sup>4</sup> It is a current pump that can produce a current as high as 1 nA,<sup>6,8</sup> but whose accuracy is not yet sufficient for a quantum current standard.

A schematic picture of the balanced SQUID is presented in Fig. 1(a). It or any other system of  $n$  JJs in parallel forming  $n-1$  loops can be modeled as follows. The current through the junction  $i$  is  $I_i = I_{ci} \sin \phi_i$ , where  $I_{ci}$  and  $\phi_i$  are the critical current and the phase of the JJ, respectively. The total current is the sum of  $I_i$ . The magnetic fluxes of the loops can be written as an  $n-1$  dimensional vector  $\Phi_{\text{tot}} = \Phi - \mathbf{L}\mathbf{I}$ , where  $\Phi = (\Phi_1 \dots \Phi_{n-1})^T$  are the external magnetic fluxes and  $\mathbf{I} = (I_1 \dots I_n)^T$ . The  $(n-1) \times n$  inductance matrix  $\mathbf{L}$  contains the coefficients  $L_{ji}$  which determine the magnetic flux induced to the loop  $j$  by the current  $I_i$ . The magnetic fluxes set constrictions on the phases over the JJs:  $\phi_j - \phi_{j+1} = (2\pi/\Phi_0)\Phi_{\text{tot},j}$ , where  $\Phi_0$  is the flux quantum.

In the limit of zero inductances, the total current is obtained in an analytic form  $I = I_{c1} \sin(\phi_1) + I_{c2} \sin(\phi_1 - f_1)$

$+ \dots + I_{cn} \sin(\phi_1 - f_1 - \dots - f_{n-1})$ , where  $f_j = 2\pi\Phi_j/\Phi_0$ . The critical current of the whole structure  $I_c(f_1, \dots, f_{n-1})$  as a function of the magnetic fluxes can be solved with the help of trigonometric identities. The full model including the inductances requires extensive computation over the phases of the JJs, whereas the analytic model allows direct calculation of the critical current. Therefore, the analytic zero-inductance model is helpful for the analysis and parameter fitting of the measurement results when the inductances are small.

Since we are interested in the suppression of a critical current that is originally of the order of tens of nanoamperes, we must be able to measure the critical current at least at 0.1 nA level. So low currents belong to the regime of phase diffusion, where a current-voltage ( $IV$ ) measurement gives a maximum supercurrent roughly proportional to  $I_c^2$ . Moreover, the result is very sensitive to the electromagnetic environment.<sup>9</sup> Even a  $IV$  measurement of a critical current of about 50 nA requires a special environment.<sup>10</sup> Therefore, we add a detector junction with  $I_{c4} > 100$  nA in parallel with our

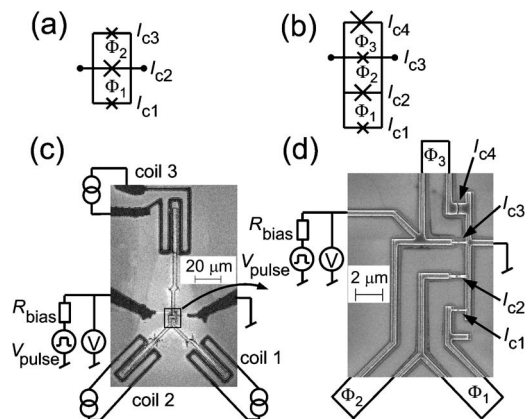


FIG. 1. (a) Balanced SQUID. The middle junction is larger than the others. (b) Large detector junction in parallel with the balanced SQUID. (c) Scanning electron micrograph of the sample showing the on-chip coils and the narrow SQUID loops, and a simplified sketch of the measurement setup. Here, the resistance in series with the pump is  $R_{\text{bias}} = 100$  k $\Omega$ . (d) Magnified view of the junctions and a sketch of the SQUID loops.

<sup>a)</sup>Electronic mail: antti.kemppinen@mikes.fi.

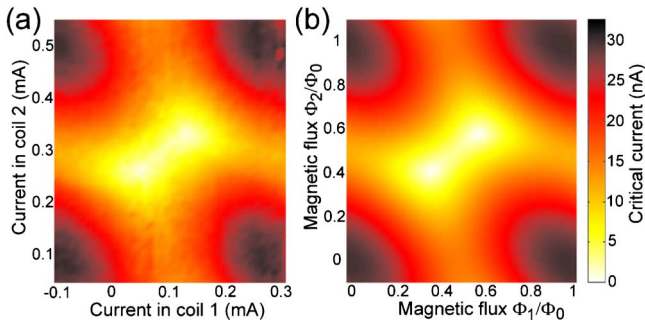


FIG. 2. (Color online) (a) Measured critical current  $i_{cb}$  of the balanced SQUID as a function of the coil currents. The maximum is shifted from zero current due to an offset flux. (b) Respective theoretical flux modulation of the critical current calculated with the parameters fitted from the measurement.

balanced SQUID, see Fig. 1(b). This superconducting shunt protects the balanced SQUID from the environment. The critical current of the four-junction system exhibits sinusoidal modulation around  $I_{c4}$  as a function of the flux  $\Phi_3$ . The amplitude of the modulation equals the critical current of the balanced SQUID.

The sample presented in Fig. 1 was fabricated by standard electron beam lithography and two-angle evaporation on oxidized silicon wafer. Aluminum was used as the superconductor and aluminum oxide as the tunnel barriers. The lateral size of the barriers was roughly  $160 \times 60 \text{ nm}^2$  for junction 2 and  $90 \times 60 \text{ nm}^2$  for junctions 1 and 3. The SQUID loops were designed narrow but rather long. In this way, the coils couple effectively to the corresponding loops with small crosstalk, but the loop inductances are relatively small.

We measure switching into the normal state to determine the critical current at a certain magnetic flux set  $\Phi$  by feeding current pulses of constant length and variable height through the device. Switching produces a voltage pulse. We measure the switching probability at typically 5 points and determine the current  $I_{50}$  at which the system has a 50% probability to switch to the normal state. At the measurement temperature 125 mK, with  $I_{c4} \approx 200 \text{ nA}$  and with about 1 ms pulse lengths,  $I_{50} = \alpha I_{c4}$ , where the factor  $\alpha$  is between 0.6 and 0.7.<sup>11</sup> To distinguish between the real critical currents and the measured values obtained from the switching experiments, we use the notation  $i_{ci} = \alpha I_{ci}$  for the measured critical currents. Here the index  $i$  refers to an individual JJ or to the balanced SQUID.

The measured flux modulation of the critical current is presented in Fig. 2(a). For each data point of the 2D chart, we measured  $I_{50}$  for 11 different currents in coil 3 mapping about one flux quantum in  $\Phi_3$ . The critical current  $i_{cb}$  of the balanced SQUID was extracted from the difference of the maximum and minimum critical current of the whole structure as a function of the current in coil 3.

The critical currents of junctions 1 and 3 are almost equal in our balanced SQUID design, see Fig. 1. Junction 2 is larger. The critical current of the SQUID is tunable to zero if  $I_{c2} \leq I_{c1} + I_{c3}$ . The flux modulation of the SQUID is periodic in the square with  $\Phi_1, \Phi_2 \in (0, \Phi_0)$ , see Fig. 2. The critical current has the maximum value at the corners of the square. In the middle region, there are two minima. If  $I_{c2} \geq I_{c1} + I_{c3}$ , there would be only one minimum with value  $I_{c2} - (I_{c1} + I_{c3})$ . The two minima are close to the line  $(0, 0)$

$\rightarrow (\Phi_0, \Phi_0)$ . In the Cooper pair sluice, one could use a coil coupled symmetrically to the loops instead of the individual couplings exploited here. It would then be possible to move along the direction  $(0, 0) \rightarrow (\Phi_0, \Phi_0)$  from the minimum close to the maximum with a single rf control. An asymmetrically coupled dc controlled coil would also be required, but dc signals are easier to implement.

We fitted the zero-inductance model to the entire 3D flux modulation data. As fitting parameters, we used the critical currents of the junctions  $i_{ci}$ , the offset flux vector  $\Phi_{\text{offset}}$  and the matrix  $\mathbf{K}$  depicting the couplings and cross couplings between the coils and the SQUID loops,  $\Phi = \Phi_{\text{offset}} + \mathbf{K}\mathbf{I}_{\text{coil}}$ . The fitted parameters were used to calculate the theoretical flux modulation chart presented in Fig. 2(b). The resulting critical currents are  $i_{c1} = 7.4 \text{ nA}$ ,  $i_{c2} = 13.5 \text{ nA}$ ,  $i_{c3} = 9.0 \text{ nA}$ , and  $i_{c4} = 142.5 \text{ nA}$ . The maximum critical currents of the balanced SQUID and the whole structure are about 30 and 172 nA, respectively.

Next, we performed a measurement at  $17 \times 17$  points near the minimum of the critical current of the balanced SQUID with about  $\Phi_0/400$  step in  $\Phi_1$  and  $\Phi_2$ . Since the coupling of the detector coil 3 to the balanced SQUID loops is expected to have the most pronounced effect near the minimum, we fitted the terms  $K_{13}$  and  $K_{23}$  of the flux coupling matrix again to these data. The flux coupling matrix combined from the two fits is

$$\mathbf{K} = \begin{pmatrix} 2.52 & 0.09 & 0.10 \\ 0.04 & 2.39 & 0.11 \\ 0.05 & 0.06 & 2.63 \end{pmatrix} \Phi_0/\text{mA}. \quad (1)$$

The cross coupling terms  $K_{13}$  and  $K_{23}$  are somewhat larger than expected, partly because the bonding wires of coil 3 pass near the sample. This enhances the effect that the fluxes  $\Phi_1$  and  $\Phi_2$  do not remain constant when the flux sweep over  $\Phi_3$  is being performed.

One of the measured flux modulation curves with respect to the detector coil 3 is shown in Fig. 3 by open circles. The chosen curve corresponds to the measurement point  $(\Phi_1, \Phi_2)$  that is closest to the fitted minimum of the critical current of the balanced SQUID. Due to the cross coupling, the lowest critical currents cannot be directly extracted from the modulation amplitude. The zero-inductance model gives the modulation curve shown by the black line and a critical current 0.035 nA at this measurement point.

The parameter fits were performed to data extending over one flux quantum in the detector loop. To test the validity of our model, we extrapolated the fits over four periods in  $\Phi_3$  and compared to the measurements. The theoretical predictions and the measured data at two  $(\Phi_1, \Phi_2)$  points near the minimum are shown in Fig. 3. The only fitting parameter was the overall magnitude of each data set. The deviations of the measurement points from the theoretical curves are less than about 0.2 nA and no systematics of the deviations is observed.

The remaining sources of residual critical current in the balanced SQUID are noise and the inductances of the loops. The effect of the inductance  $L$  is proportional to the magnetic flux that a current circulating in the loop can produce:  $2\pi L I_{ci} / \Phi_0$ . This effect can be dominating with large JJs, which can be fabricated with smaller relative parameter scatter. Hence the balanced SQUID does not outperform the dc SQUID in that case.

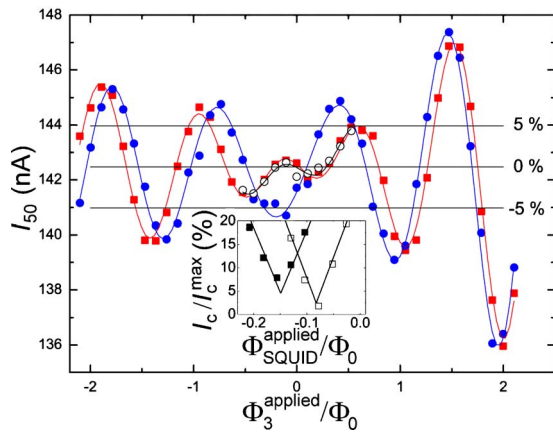


FIG. 3. (Color online) Detector flux modulations ( $\Phi_3^{\text{applied}} = K_{33} I_{c4}$ ) near the minimum of  $i_{c4}$ . The horizontal lines present change from  $i_{c4}$  as a percentage of the maximum of  $i_{c4}$ . The open circles are an example of the data used for the parameter fits of the cross coupling terms  $K_{13}$  and  $K_{23}$ . The black line is the corresponding curve of the zero-inductance model yielding a critical current  $i_{c4} = 0.035$  nA. The data spanning four flux quanta presented by the red squares and the blue circles were not used for fitting. The corresponding red and blue lines are the predicted flux modulations yielding  $i_{c4} = 0.17$  nA and  $i_{c4} = 1.8$  nA, respectively. The inset shows typical results of similar critical current measurements of two ordinary dc SQUIDs, expressed as a function of the applied magnetic flux of the SQUID. The minima of the critical currents are 2.5% and 4.6% of the maxima, which are about 30 nA for both SQUIDs.

The inductances of the SQUID loops consist of geometric and kinetic inductances. The geometric inductances were calculated with the superconducting version of FASTHENRY.<sup>12</sup> The kinetic inductance of a superconductor is  $L_K \approx \hbar R_N / \pi \Delta$ , where  $R_N$  is the normal-state resistance of the loop and  $\Delta$  is the BCS gap. By assuming the resistivity of the aluminum loops to be  $\rho \approx 2.7 \mu\Omega \text{ cm}$ , we get the total inductance matrix,

$$\mathbf{L} = \begin{pmatrix} 113 & -9 & 0 & 0 \\ 115 & 124 & -5 & 0 \\ 0 & 0 & 3 & -157 \end{pmatrix} \text{pH}. \quad (2)$$

Here, we have neglected the cross coupling terms except  $L_{21}$ , which is large due to the physical position of current injection to the structure, as shown in Fig. 1.

We simulated the flux modulations of the critical current with inductances from  $\mathbf{L}$  of Eq. (3) up to  $20\mathbf{L}$ , and with or without the detector junction. The critical current suppression ratio of the balanced SQUID is about 500 with  $\mathbf{L}$  and about 350 with  $2\mathbf{L}$ . In the four-junction model, increasing the inductance to  $5\mathbf{L}$  or higher breaks the simple sinusoidal modulation, and the modulation amplitude is increased. Such effects were not observed in our measurements, which supports the estimated values of the inductances.

Noise is expected to round off the apparent critical current suppression. An obvious noise source is the global magnetic field, which was diminished by a high  $\mu$  and a superconducting shield. In low- $T_c$  SQUIDs, the main  $1/f$  noise sources are the critical-current fluctuations and magnetic flux noise related to defects close to the superconducting loop lines.<sup>13</sup> Our measurement is, however, relatively insensitive to magnetic flux noise even at the minima of the critical current of the balanced SQUID, since the phase of the  $\Phi_3$  modulation gets all possible values around these points. Thus, in the first order, the modulation caused by the noise averages to zero. The rounding effect was not observed at the critical current suppression values obtained in our measurements.

In conclusion, we have demonstrated experimentally that the critical current of the balanced SQUID agrees well with the zero-inductance model. This is supported by theoretical estimation of the effect of the inductances. A conservative estimate for the critical current suppression factor is 300 or more. This number is an order of magnitude higher than the typical values obtained for two-junction dc SQUIDs with similar maximum critical currents. Furthermore, the suppression ratio does not essentially depend on the exact critical currents of the individual junctions, and hence the fabrication yield is high.

We acknowledge the Finnish Academy of Science and Letters, Väisälä foundation, Technology Industries of Finland Centennial Foundation, and the Academy of Finland for financial support.

<sup>1</sup>Y. Nakamura, Yu. A. Pashkin, and J. S. Tsai, *Nature (London)* **398**, 786 (1999).

<sup>2</sup>Yu. Makhlin, G. Schön, and A. Shnirman, *Rev. Mod. Phys.* **73**, 357 (2001).

<sup>3</sup>L. Faoro, J. Siewert, and R. Fazio, *Phys. Rev. Lett.* **90**, 028301 (2003).

<sup>4</sup>A. O. Niskanen, J. P. Pekola, and H. Seppä, *Phys. Rev. Lett.* **91**, 177003 (2003).

<sup>5</sup>M. Cholascinski, *Phys. Rev. B* **69**, 134516 (2004); *Phys. Rev. Lett.* **94**, 067004 (2005).

<sup>6</sup>A. O. Niskanen, J. M. Kivioja, H. Seppä, and J. P. Pekola, *Phys. Rev. B* **71**, 012513 (2005).

<sup>7</sup>T. Hime, P. A. Reichardt, B. L. T. Plourde, T. L. Robertson, C.-E. Wu, A. V. Ustinov, and J. Clarke, *Science* **314**, 1427 (2006).

<sup>8</sup>J. J. Vartiainen, M. Möttönen, J. P. Pekola, and A. Kemppinen, *Appl. Phys. Lett.* **90**, 082102 (2007).

<sup>9</sup>G.-L. Ingold, H. Grabert, and U. Eberhardt, *Phys. Rev. B* **50**, 395 (1994).

<sup>10</sup>A. Steinbach, P. Joyez, A. Cottet, D. Esteve, M. H. Devoret, M. E. Huber, and J. M. Martinis, *Phys. Rev. Lett.* **87**, 137003 (2001).

<sup>11</sup>J. M. Kivioja, T. E. Nieminen, J. Claudon, O. Buisson, F. W. J. Hekking, and J. P. Pekola, *Phys. Rev. Lett.* **94**, 247002 (2005).

<sup>12</sup>See <http://www.fastfieldsolvers.com> for more information.

<sup>13</sup>R. H. Koch, D. P. DiVincenzo, and J. Clarke, *Phys. Rev. Lett.* **98**, 267003 (2007).